COMPUTING OF PID PARAMETERS USING TECOMAT FOXTROT AND THE ASYMMETRICAL RELAY SHIFTING

Jakub Vaněk[1], Jan Slabý [2]

[1] Department of Instrumentation and Control Engineering, Czech Technical University in Prague
Prague, Czech Republic
Jakub.Vanek@fs.cvut.cz
[2] Department of Instrumentation and Control Engineering, Czech Technical University in Prague
Prague, Czech Republic
Jan.Slaby@fs.cvut.cz

Abstract: This paper describes the implementation of the relay shifting method for model identification and determining of PID parameters for practical use in process control. For the purpose of this paper, the programmable logic controller Tecomat Foxtrot was used together with the Mosaic development environment. The whole process consists of approximating a controlled system with a second order time delayed model called a SOTD model using the relay shifting method. The PID parameters are then determined from a SOTD model and are used for process control. Emphasis is put on the possibility of simple and effective practical implementation, which enables quick and sufficiently precise determination of the PID parameters for system control. The outcome of this work is the PLC project library together with an easy-to-use function block diagram with a built-in PID controller. The advantage of this method is its versatility, which enables its use even for systems with time delay. A demonstration of this method is given using simulated model as well as real laboratory systems.

Keywords: system control, model identification, PID parameters, autotuning

1. Introduction

Due to rapidly expanding automatization in every industrial sector, great focus is put on fast and sufficiently precise implementation and settings of individual parts of the systems. PID regulators play a large role in industrial automatization. Settings of these regulators might be time consuming and may not offer satisfying results. PID regulators are quite robust, therefore the process can be relatively well controlled, even with nonideally set parameters. However, this might bring extra financial cost, such as higher energy consumption or decreasing lifespan of equipment. For these reasons, it is necessary to conduct further research on the issues of PID controller autotuning. In this paper the application of the relay shifting method for model identification and PID tuning is presented. The method is implemented into PLC Tecomat Foxtrot (Teco a.s, Kolín, Czech Republic).

2. System identification

The first step of the presented method is the identification of the controlled system and its approximation using a SOTD model. Firstly, using the shifting method described in [1], two points of process frequency response $G(j\omega_1)$ and $G(j\omega_2)$ are determined (see Fig. 1). Based on the knowledge of these two points, the second step is the approximation of the system in the form of a SOTD model using the Least Squares Method.

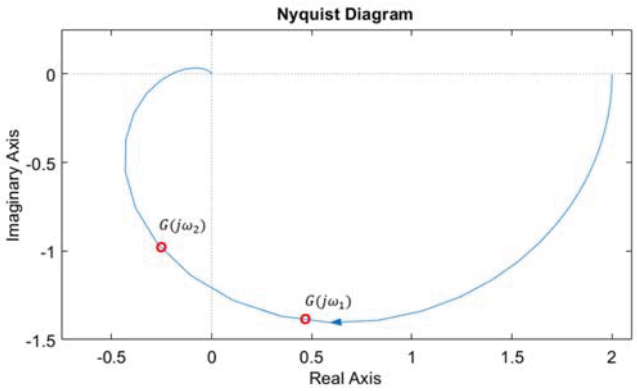

Fig. 1. The Nyquist frequency characteristic with two determined points

2.1 Relay Shifting Method

This method, presented in [1], is based on the use of asymmetrical relay for process control in the proximity of the operating point. A stable oscillation with period T_p after the stabilization time of T_L is prerequisite. Fundamental frequency can be determined by:

$$\omega_1 = 2\pi/T_p \tag{1}$$

and the second harmonic:

$$\omega_2 = 2\omega_1 \tag{2}$$

For the purpose of using this method in real-world systems, T_L is considered to be the time after which 3 subsequent oscillations take place. These meet the following criteria:

- Difference from mean of 3 consequential periods must be lower than 10%.
- Difference from mean of maximal *y* values from 3 consequential periods must be lower than 10%. Where *y* is the system output value.
- Difference from mean of minimal *y* values from 3 consequential periods must be lower than 10%.

The first point is calculated as [1]:

$$G_{(j\omega_1)} = \frac{\int_t^{t+T_p} y(\tau) e^{-j\omega_1\tau_d} d\tau}{\int_t^{t+T_p} u(\tau) e^{-j\omega_2\tau_d} d\tau} \tag{3}$$

The second point is determined as [1]:

$$G_{(j\omega_2)} = \frac{\int_t^{t+T_p} \left(y(\tau) + y\left(\tau - \frac{T_p}{2}\right) \right) e^{-j\omega_2\tau_d} d\tau}{\int_t^{t+T_p} \left(u(\tau) + u\left(\tau - \frac{T_p}{2}\right) \right) e^{-j\omega_2\tau_d} d\tau} \tag{4}$$

Where *u* is the manipulated variable. The approximating SOTD model is then identified in the form of [1]:

$$M_{(s)} = \frac{K \cdot e^{-s\cdot\tau_d}}{a_2 \cdot s^2 + a_1 \cdot s + 1} \tag{5}$$

Which can be rearranged for non-oscillating systems into the form:

$$M_{(s)} = \frac{K \cdot e^{-s\cdot\tau_d}}{(T_1 \cdot s + 1) \cdot (T_2 \cdot s + 1)} \tag{6}$$

2.2 Computing transition parameters using Least Squares Method

The Least Squares Method is used to determine the parameters K, a_2 and a_1 from the (5) equation. The term $e^{-s\cdot\tau_d}$ element in equation (5) is represented by the Euler formula. By the equation (5) and the points $G(j\omega_1)$ and $G(j\omega_2)$ and the subsequent decomposition into real and imaginary parts, we obtain the equation (7), see [4]:

$$\boldsymbol{Z}\cdot\boldsymbol{\theta}=\boldsymbol{\varsigma} \tag{7}$$

where:

$$\boldsymbol{Z}=\begin{bmatrix}\cos(\omega_1\cdot T_d) & R_1\cdot\omega_1^2 & I_1\cdot\omega_1\\ -\sin(\omega_1\cdot T_d) & I_1\cdot\omega_1^2 & -R_1\cdot\omega_1\\ \cos(\omega_2\cdot T_d) & R_2\cdot\omega_2^2 & I_2\cdot\omega_2\\ -\sin(\omega_2\cdot T_d) & I_2\cdot\omega_2^2 & -R_2\cdot\omega_2\end{bmatrix}, \tag{8}$$

$$\boldsymbol{\theta}=\begin{bmatrix}K\\ a_2\\ a_1\end{bmatrix}, \tag{9}$$

$$\boldsymbol{\varsigma}=\begin{bmatrix}R_1\\ I_1\\ R_2\\ I_2\end{bmatrix}. \tag{10}$$

R_1, R_2 are real parts of points $G(j\omega_1)$ and $G(j\omega_2)$. And I_1, I_2 are imaginary parts of these points.

The known maximum time delay T_{Dmax} is divided into 500 parts, for each of which a calculation is conducted using the Least Squares Method. T_{Dmax} is estimated as the mean of possible time delays T_{d1}, T_{d2}, T_{d3} (see Fig. 2) increased by 10% to minimize possible error.

$$\boldsymbol{\theta}=(\boldsymbol{Z}^{\boldsymbol{T}}\cdot\boldsymbol{Z})^{-1}\boldsymbol{Z}^{\boldsymbol{T}}\cdot\boldsymbol{\varsigma} \tag{11}$$

By applying the criterion “Sum of the squared residuals” determined according to:

$$Kr=\boldsymbol{E}^{\boldsymbol{T}}\cdot\boldsymbol{E}, \tag{12}$$

where:

$$\boldsymbol{E}=\varsigma-\boldsymbol{Z}\cdot\boldsymbol{\theta}. \tag{13}$$

The desired solution must meet the following conditions: $a_2 > 0$, $a_1 > 0$. These conditions are valid for a stable system.

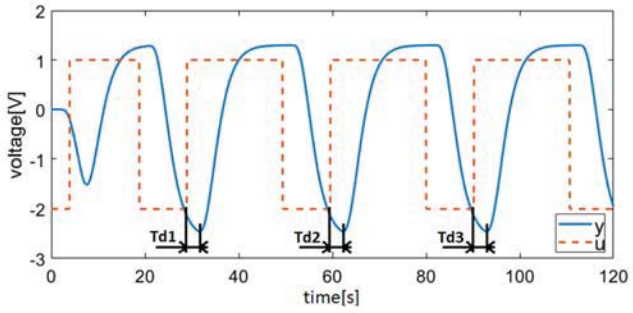

Fig 2. Possible Time delays

2.3 PID Tuning Methods

The identified mathematical model (5) is used to determine the PID parameters of the regulator in use. To ensure versatility, 3 methods of regulator tuning are used. For the purpose of optimization regarding the speed of PLC computing, emphasis is put on simplicity of the calculation. The method described in *3.1 or 3.3* are used for systems

with time delay, based on PID parameter suitability. For systems identified without time delay, the used method is 3.2. The PID controller is described by the formula (25).

2.4 PMC – Phase margin criteria for models with time delay

Based on the identified parameters $K, \tau_d, a_2$and a_1, it is possible to determine the parameters of PID regulators for a time delay system in the following manner [2]:

$$r_i = \frac{\pi}{4 \cdot |K| \cdot \tau_d} \tag{14}$$

$$r_0 = a_1 \cdot r_i \tag{15}$$

$$r_d = a_2 \cdot r_i \tag{16}$$

2.5 PMC – Phase margin criteria for models without time delay

This method is suitable for system in form (5) identified without a time delay. Determined parameters are [4]:

$$r_i = \frac{1}{T_w \cdot K}, \tag{16}$$

where T_w is wanted time constant and was chosen as

$$T_w \leq \frac{1}{\left| Re\left(\frac{-a_1 + \sqrt{a_1^2 - 4 \cdot a_2}}{2 \cdot a_2} \right) \right|}. \tag{17}$$

$$r_0 = a_1 \cdot r_i \tag{18}$$

$$r_d = a_2 \cdot r_i \tag{19}$$

2.6 SIMC tuning method

This method is suitable for non-oscillatory time delayed model in form of (6). Determined parameters of PID regulators are [2]:

$$r_0 = \frac{0{,}5 \cdot (T_1 + T_2)}{K \cdot \tau_d} \tag{20}$$

$$T_i = T_1 + T_2 = a_1 \tag{21}$$

$$T_d = \frac{T_2}{1 + \frac{T_2}{T_1}} \tag{22}$$

where

$$T_i = \frac{r_0}{r_i} \tag{23}$$

$$T_d = \frac{r_d}{r_0} \tag{24}$$

3. Implementation

Implementation is carried out in the Mosaic programming environment for PLC Tecomat Foxtrot. It is divided into three parts. The principles of the first two parts – identification and calculation – are explained in chapters *2* and *3*. The third part is feedback control. During programming, emphasis was put on speed of calculation with regard to PLC performance, and also on user-friendliness, specifically on easy implementation into PLC code. The identification and calculation parts are carried out only once. After that, the PLC switches to the control part, where it remains until manual reset.

The user can utilize the PLC program in the form of function block diagram (see Fig. 3), where it is necessary to enter the input parameters.

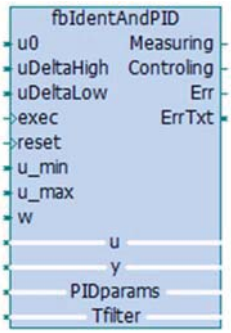

Fig. 3. Function block in Function block diagram

Where:

- u_0 is the input manipulated value for the operating point
- *uDeltaHigh* and *uDeltaLow* are relay deviations from the operating point
- *u_min* and *u_max* are limitations for input saturation
- *exec* starts the program.

The identification part consists of a state machine with three states. In the first phase, resetting of variables is ensured. In the second phase, the stabilized value of the output quantity in the operating point is deducted. The third phase is the measuring itself. The values of the input *u* and the output *y* are saved in periods into memory buffers every 20 ms. This sampling period was set as lowest safe time considering the PLC's cycle time. In the event of buffer overflow, the sampling period is automatically adjusted. After the criteria are fulfilled for 3 consecutive periods as described in chapter *2.1*, the identification part is complete. With regard to the PLC registry memory, only the last three periods are retained.

In the calculation part, the calculation of points from chapter *2.1*, deduction of T_{Dmax}, and subsequently the calculation of the SOTD model using the Least Squares Method from chapter *2.2* take place. After that, the PID parameters for the regulator are determined as described in chapter *3*. Since the PLC has a limited computing performance and, at the same time, must control processes in other technologies, the most straightforward calculations were chosen, especially when determining the PID parameters. The constant N for the PID regulator (25) is set to 10 as recommended in [3] and the time constant T_f for the first order filter (26) is then also determined in this part. The filter is put into operation during the start of the control part. It was implemented into the controlling to optimize the course of the output quantity *y*. After the computing part is completed, buffers and other calculated parameters are uploaded to an SD card for further analysis and the PLC switches to the control part, where inbuilt blocks of the PID regulator and first order filter are utilized.

$$U(s) = r_0 \cdot E(s) + \frac{1}{s \cdot T_i} \cdot E(s) - \frac{r_d \cdot s}{\frac{1}{N} \cdot s + 1} \cdot Y(s) \tag{25}$$

$$M_f(s) = \frac{1}{T_f \cdot s + 1} \tag{26}$$

In Fig. 4, the functional block of the controlling part is depicted using a Simulink scheme.

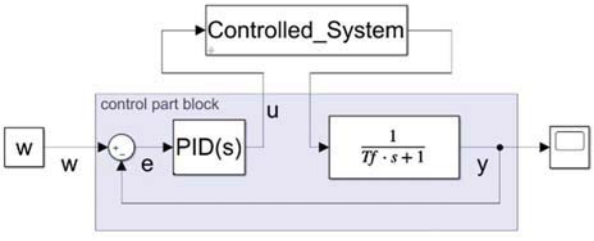

Fig. 4. Controlling part of Function block

4. Experiments

The presented method has been successfully tested on several simulated systems, one of which will be presented here. The tests were also performed using an actual laboratory apparatus.

4.1 Simulated experiment

The test was conducted on a system using the following transfer function:

$$M_{S1} = \frac{2}{(s+1)\cdot(1.5\cdot s+1)\cdot(2\cdot s+1)} \tag{27}$$

The system (27) was used in Tecomat Foxtrot simulation mode with results presented in Fig. 5,

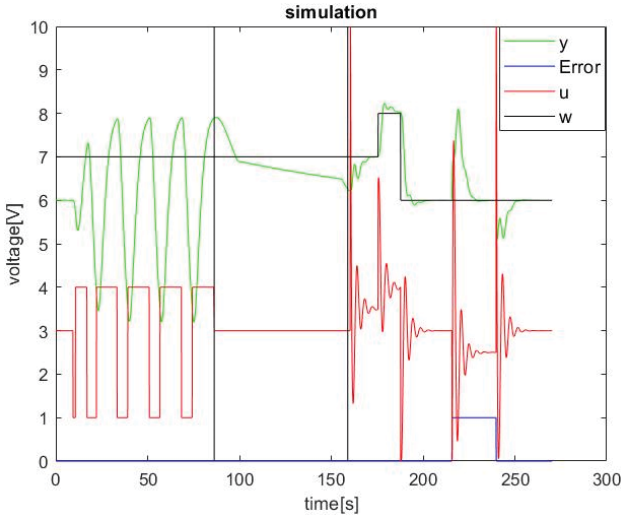

Fig. 5. Course of model identification and process control

Where:

- *y* is the controlled variable
- *Error* is the simulated disturbance
- *u* is the manipulated variable
- w is the desired variable

The process in Fig. 5 is separated into 3 sections by horizontal lines at the times of 86s and 156s. In the first section, system identification using asymmetrical relay takes place. In the second section, the calculation part takes place where two points of frequency response are determined based on the measurement from the first section, then the model in the form of (5) is calculated. Based on this model, the PID parameters are determined. In the third section, feedback process control takes place. After the stabilization of *y* on the desired variable *w* at the time of 175s, the desired variable *w* increases from 7 Volts to 8 Volts and, at the time of 188s, it decreases to 6 Volts. At the time of 216s, the disturbance *Err* will appear for the following 20 seconds. It is evident that the variable *y* is controlled successfully as it always stabilizes at the desired variable *w*.
The transfer function (28) was identified as an approximation of the simulated system.

$$M_{(j\omega)} = \frac{1.91\cdot e^{-j\cdot\omega\cdot 0.48}}{4.61\cdot(j\cdot\omega)^2 + 3.76\cdot j\cdot\omega + 1} \tag{28}$$

The original transfer function (27) is then compared with its identified approximation (28) in Fig. 6.

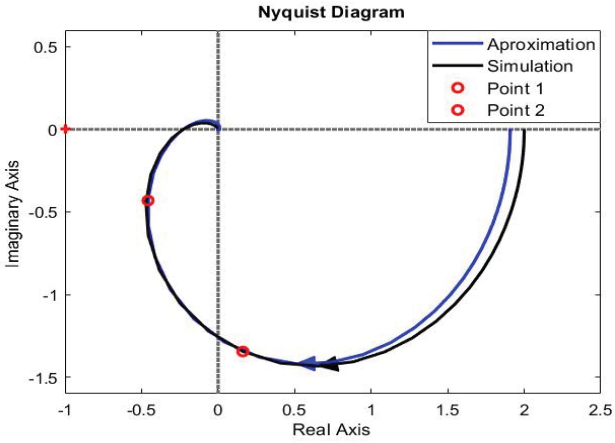

Fig. 6. The Nyquist frequency characteristic comparation for simulated system and its approximation.

According to Fig. 6, it is evident that the approximation (28) describes the simulated system (27) precisely enough and it is possible to use this approximation for PID parameter determination.
The PID parameters were calculated based on calculations described in chapter *3*. Based on equations (14), (15) and (16) the results are: r_0=3.23 r_i=0.86s^{-1} and r_d=3.95s.

4.2 Experiments produced on real systems

For testing purposes, the laboratory apparatus called “air aggregate” (see Fig. 7) was used in two different settings.

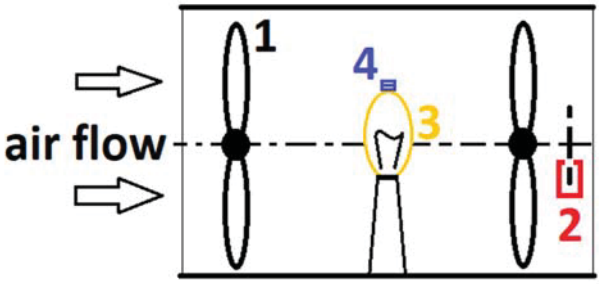

Fig. 7. The laboratory apparatus “Air aggregate”. 1-fan, 2-flow meter, 3-light bulb, 4-thermistor

For the first test, the airflow setting was used where the manipulated variable *u* is the voltage on the fan and the controlled variable *y* is the voltage on the flow rate meter. For the second test, the heating setting was used where the manipulated variable *u* is the voltage on the light bulb and the controlled variable *y* is the voltage on the thermistor. The fan is used as a disturbance for the second test.

In Fig. 8, the courses of presented method used on air aggregate in airflow mode are presented. The controlled variable *y* is the voltage on the flow meter, *Error* is the simulated disturbance on variable *y*, *u* is the manipulated variable and *w* is the desired variable. The process in Fig. 8 is separated into 3 sections by horizontal lines at the times of 236s and 309s. In the first section, system identification using asymmetrical relay takes place. In the second section, the calculation part takes place where two points of frequency response are determined based on the measurements from the first section, then the model in the form of (5) is calculated. Based on this model, the PID parameters are determined. In the third section, feedback process control takes place. The identification section takes longer than during the simulated experiment because of the conditions described in section A of chapter *III*. were met after 12 periods. It is apparent that in the feedback control section, the system was controlled successfully.

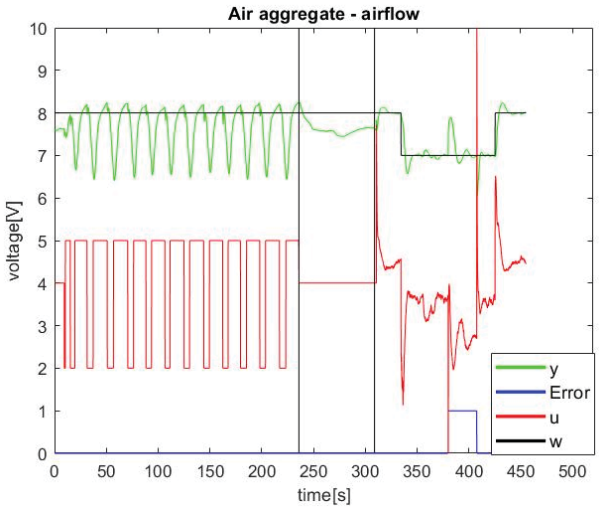

Fig. 8. Course of model identification and process control of the air aggregate with airflow setting.

Results of the test carried out using the Air aggregate laboratory apparatus with heating settings are presented in Fig. 9.

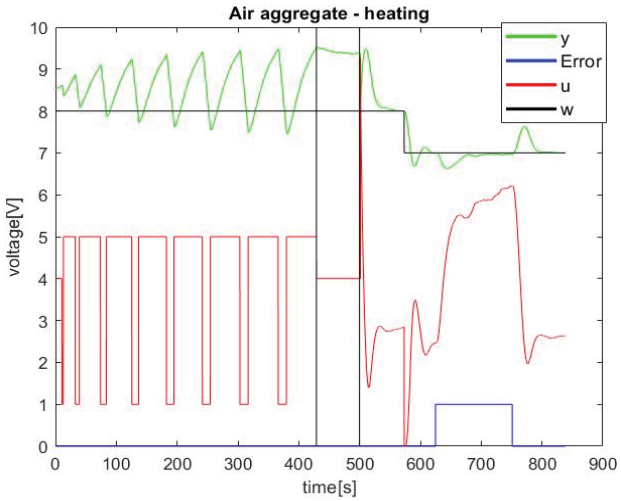

Fig. 9: Course of model identification and process control of the air aggregate with heating setting

The controlled variable *y* is the voltage on the light bulb, *Error* is the voltage on the fan creating disturbance, the manipulated variable *u* is the voltage on the thermistor and *w* is the desired variable. From Fig. 9 it is evident that the apparatus was successfully identified and controlled.
The duration period is affected by system speed and process stability. The simulated system was identified fastest because the system is not burdened by disturbances, therefore the conditions for measuring termination described in section A of chapter *2*. were met immediately.

5. Conclusion

Although it is necessary to further test the procedure before implementation in practice, as well as complete the error handling system, it is possible to state that this procedure has potential for practical use. Tests were conducted on a simulated system of 3rd order and on two actual laboratory apparatuses, where the system was successfully identified, the PID parameters were determined and, subsequently, the system was successfully controlled. The next focus will concentrate on testing and the eventual changes in determining PID parameters to ensure the highest possible versatility of use. Time will also be given to ensure automatic settings of sampling time regarding PLC

cycle time. The next steps for accuracy improvement and higher versatility will be carried out in the identification part.

Acknowledgment

This work was supported by the Grant Agency of the Czech Technical University in Prague, grant No. SGS19/158/OHK2/3T/12.

References

[1] M. Hofreiter, "Improved relay feedback identification using shifting method," in Proceedings of the 16th International Conference on Informatics in Control, Automation and Robotics (ICINCO 2019). Madeira: SciTePress, 2019. p. 601-608. ISBN 978-989-758-380-3.

[2] A. Hornychová a M. Hofreiter. Use of the shifting method results for PID controllers parameters estimation. MATEC Web of Conferences. 2019, 292, 01017. DOI: 10.1051/matecconf/201929201017.

[3] M. Vítečková and A. Víteček, "Vybrané metody seřizování regulátorů," Vysoká Škola Báňská - Technická Univerzita Ostrava, 2011.

[4] M. Hofreiter. Personal consultation, author of The relay shifting method 2020.

Selected article from
Tento dokument byl publikován ve sborníku

Nové metody a postupy v oblasti přístrojové techniky, automatického řízení a informatiky 2020

New Methods and Practices in the Instrumentation, Automatic Control and Informatics 2020

14. 9. – 16. 9. 2020, Zámek Lobeč

ISBN 978-80-01-06776-5

Web page of the original document:
http://iat.fs.cvut.cz/nmp/2020.pdf

Obsah čísla/individual articles:
http://iat.fs.cvut.cz/nmp/2020/

Ústav přístrojové a řídicí techniky, FS ČVUT v Praze, Technická 4, Praha 6